RSC Advances

ROYAL SOCIETY OF CHEMISTRY

www.rsc.org/advances

Journal Name

RSCPublishing

ARTICLE

pH-Responsive Drug Release from Porous Zinc Sulfide Nanospheres based on Coordination Bonding

Cite this: DOI: 10.1039/xoxxoooooox

Dong Zhu,* Hong-Mei Wen,* Wei Li, Xiao-Bing Cui, Li Ma and An Kang

Received ooth January 2012,
Accepted ooth January 2012

DOI: 10.1039/xoxxoooooox

www.rsc.org/

pH-responsive systems have attracted special research interest in drug delivery. Herein, we report a pH-responsive system based on the "COOH-Zn^{2+}-drug" architecture via coordination bonding in ZnS nanospheres mesopores. PAA-functionalized porous ZnS nanospheres were employed as cargo carriers for hosting metal ion (Zn^{2+}) binders and drug molecules to form the "COOH-Zn^{2+}-drug" architecture. The cleavage of either the "COOH-Zn^{2+}" or the "Zn^{2+}-drug" coordination bond, in response to pH variations, gives rise to a significant release of drug molecules under weakly acidic conditions (pH 5-6.5). We anticipate that the porous ZnS nanospheres and subsequently prepared pH-responsive system may prove to be a significant step toward the development of a finely pH-sensitive drug delivery system that minimizes drug toxicity.

Introduction

In cancer therapy, adverse side effects and collateral damage are almost inevitable because traditional anticancer drugs cannot distinguish between cancerous and healthy cells. To address this formidable challenge, diverse classes of controlled drug delivery systems (CDDS) have been widely investigated to enhance the drug delivery efficiency, reduce toxicity and side effects and improve patient convenience.[1-4] Up to date, many materials, e.g., liposomes,[1] dendrimers,[2] block copolymers,[3] and various inorganic nanomaterials,[4] have been utilized as drug carriers in CDDS. Among them, porous silica nanomaterials have emerged as robust nanovectors for drug delivery because of their remarkable biocompatibility and stability, and capacity to carry disparate payloads (molecular drugs, proteins, other nanoparticles) within the porous core.[5-7] These systems take up or release drug molecules in response to external stimuli such as pH, [8-13] light irradiation, [14-15] ionic strength, [16-17] redox potential, [18] temperature[19-20] and enzymes, [21] etc. Of these stimuli-responsive systems, pH-responsive systems have attracted special research interest[22] because they enable exploitation of the acidic environment of cancerous tissue. It is well-documented that the pH (5.7-7.2) in tumor and inflammatory tissues is more acidic than in blood and normal tissue, with endosomes and lysosomes exhibiting even lower pH values (5.0-5.5). [23] Fabrications of these pH responsive systems involve utilizing the soft matter systems such as hydrogels triggered by a swelling/deswelling effect[24] and micelles and liposomes by the stabilization/destabilization effect, [25] and plus various inorganic solids as gatekeepers including supramolecular nanovalves, pH-sensitive linkers, and polyelectrolytes.[26-29] However, it is still challenging and urgent need for practical clinical applications to design a finely pH-responsive controlled drug delivery system.

On the other hand, Zinc sulfide (ZnS) semiconductors nanoparticals have attracted widely interest for many applications such as phosphors, bioimaging, sensing, and photocatalysis.[30-35] However, ZnS nanospheres, and especially porous nanostructures, remain relatively under-explored in terms of delivery systems. Although porous silica nanospheres were the most used inorganic solids carrier in the previous reports, the functionalization of silica is usually restricted by the physical nature of silica as well as the limited number and high cost of organosiloxane reagents. More importantly, recent reports highlight the potential toxicity of silica nanoparticles due to interactions of surface silanols with cellular membranes.[36-39] Thus, development of alternative non-silica-based carriers is critical, in which porous ZnS nanospheres (PZNs) exhibited hierarchical structure with porous features, excellent colloidal stability, and good biocompatibility.[40-41]

Herein, we used a simple and facile synthetic strategy to prepare uniform-size and porous ZnS nanospheres and fabricated a pH-responsive drug release system based on the coordination bonding of metal ions (Zn^{2+}) and carboxylic functional groups (-COOH-). To the best of our knowledge, this is the first report of a pH-responsive system based on porous ZnS nanospheres. In the case of the preparation of the drug release system, plenty of carboxylic groups of Poly (acrylic acid) (PAA) were anchored onto the outer surfaces of the amine-capped ZnS nanospheres (denoted COOH-PZNs) by the amidation reaction of poly-(acrylic acid) homopolymer with amino groups on the surface of the ZnS mesopores, which afforded not only hydrophilicity but also an abundance of carboxyl groups, to effectively load the Zn^{2+} ions. Zn^{2+} is

College of Pharmacy, Nanjing University of Chinese Medicine Nanjing 210023, P. R. China
Tel: +86 25 85811839. Fax: +86 25 85811839.
*Corresponding author. Dong Zhu and Hong-Mei Wen
E-mail: dongzhunjutcm@hotmail.com; njwenhm@126.com

Electronic Supplementary Information (ESI) available: [The hydrodynamic diameter of PZNs]. See DOI: 10.1039/b000000x/

readily absorbed by carboxyl groups to form a "COOH-Zn^{2+}" coordination bond on the mesopore surface. Finally, Doxorubicin hydrochloride (DOX), a well-known chemotherapeutic drug, was bonded to the Zn^{2+} ions in the carrier to form "COOH-Zn^{2+}-DOX" architecture. A breakup of either (or both) coordination bond, triggered by a reduction in external pH, leads to the release of DOX molecules from the carrier into the surrounding environment. This route opens up a facile but powerful avenue for the design of various pH-responsive systems and new opportunities for their application in drug delivery.

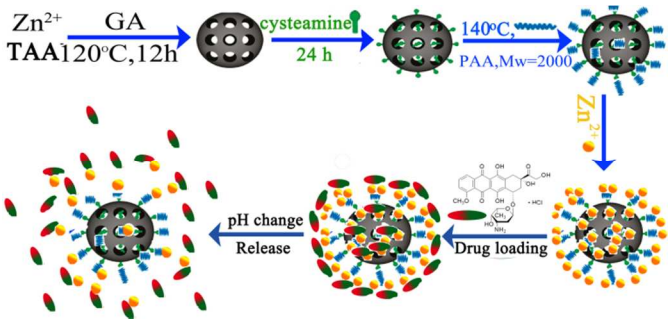

Figure 1 Schematic mechanism for the pH-Responsive drug released system based on coordination bonding in mesopores PZNs.

Experimental Section

Chemicals.

Poly(acrylic acid) (PAA, Mw = 2000) and Dimethylformamide (DMF) were purchased from Shanghai Aladdin reagent Co., Ltd. Cysteamine and Gum Arabic (GA) were purchased from Shanghai Aladdin-reagent Chemical Reagent Co., Ltd. $ZnAc_2$•$2H_2O$, $ZnCl_2$, thioacetamide (TAA) and other chemical reagents were obtained from Nanjing Chemical Reagent Co., Ltd. Doxorubicin hydrochloride (DOX) was obtained from Shanghai Sangon. Biotech.Co. All chemicals were directly used as received without further purification. Millipore water (18.2 MΩ cm at 25℃) was used throughout all of the experiments.

Preparation of COOH-PZNs.

PZNs were synthesized in one pot via a hydrothermal route, similar to previous report.[40] In a typical procedure, $ZnAc_2$•$2H_2O$ (1 mmol), GA (100 mg) and TAA (1 mmol) were dissolved in water (40 mL) in the order stated and ultrasonicated vigorously to obtain a clear solution. The mixed solution was transferred into a Teflon-line autoclave and maintained at 120 ℃ for 12 h. The white solid products were collected by centrifugation and washed at least three times with ethanol and water. They were then dried in a vacuum at 45 ℃ for 10 h. For the further surface modification, 100 mg of PZNs was redispersed in 50 mL of dehydrated ethanol and then purged with dry nitrogen for 30 min to exclude the oxygen in the ethanol. An amount of 2.5 mmol of cysteamine was dissolved into the above solution, and the mixture was stirred for 24 h in a sealed vessel. Mercapto groups of cysteamine tightly attached onto the surface of the PZNs due to the excess of metal ions with respect to sulfide ions at the surface of the nanospheres. The resultant amine-capped PZNs were centrifuged and washed with ethanol several times to remove the residue of cysteamine and drying overnight in a vacuum at 45 ℃ for 12 h to give NH_2-PZNs as white powders. Subsequently, NH_2-PZNs (30 mg) was dispersed in 10 mL of DMF, and then 10 mg of PAA (Mw = 2000) was dissolved into the mixture. The reaction mixture was stirred at 140 ℃ for 2 h. After the reaction, the mixture was centrifuged and washed with copious ethanol. To ensure that the PAA physically adsorbed on PZNs was removed completely, the washing procedure was repeated until the weight loss of PAA-PZNs (calculated by TGA) did not change. The resultant product was dried overnight in a vacuum at 45℃. The preparation of the COOH-PZNs was also shown in Figure 1.

Loading of DOX into PZNs to Form "COOH-Zn^{2+}-DOX" Architecture

Stock solutions (0.1 M) of Zn^{2+} were prepared by dissolving $ZnCl_2$ in absolute ethanol. In a typical charging process of metal ions into the PAA functionalized PZNs, 0.15 g of the PAA-PZNs were dispersed in 8 mL of the stock solution, and the mixture was stirred at ambient temperature for 2 h. Then the PAA-PZNs were recovered by centrifugation, washed 10 times with ethanol, and dried at 40 ℃ overnight. The loading amounts of Zn^{2+} ions have been calculated by contents change of Zn^{2+} stock solutions and loss amounts of washing based on ICP analysis results. DOX, a well-known anticancer drug, was chosen as a model drug to assess the drug loading and release behaviour. Typically, 50 mg of Zn^{2+}-ion-loaded PZNs were dispersed in 8.0 mL of 0.5 mM solution of DOX and ambient temperature, and further stirred for 8 h to reach the equilibrium state. After that, the DOX loaded PAA-PZNs (DOX-Zn^{2+}-PAA-PZNs) were collected by centrifugation, washed five times with 2 mL of pH = 7.4 PBS to remove the physically absorbed DOX and dried at 40 ℃ overnight. The amount of loaded drug was determined by a UV-vis spectrophotometer. The drug loading content and entrapment efficiency were calculated by the following equations:

$$\text{Loading content} = \frac{\text{Mass of drug in PZNs}}{\text{Mass of drug loaded PZNs}}$$

$$\text{Entrapment efficiency}(\%) = \frac{\text{Mass of drug in PZNs}}{\text{Initial Mass of drug}} \times 100\%$$

The way to the immobilization of Zn^{2+} and the loading of DOX into PZNs procedure are also shown in Figure 1.

Release of DOX under Different pH Conditions.

In the in vitro drug release experiment, 10 mg of the DOX-Zn^{2+}-PAA-PZNs powder was dispersed into 2 mL of deionized water. The dispersion was transferred into a dialysis bag (cut off molecular weight 7000 g • mol-1), and then the bag was immersed into 100 mL of PBS solution with different pHs (5.6, 6.2, 6.8, and 7.4) at 37℃ with magnetic stirring. An amount of 1.0 mL of solution was withdrawn at a given time interval,

followed by supplying the same volume of fresh PBS solution. The amount of released drug was measured by a UV-vis spectrophotometer.

In Vitro Cell Assay. To check cellular uptake and DOX release, HeLa cells were cultured in an 12-well chamber slide with one piece of cover glass at the bottom of each chamber in incubation medium (DMEM) for 24 h. To each Petri dish was added 100 μL of nanoparticles with "DOX-Zn^{2+}-PAA-PZNs" architecture (0.5 mg, loading of DOX: 61 mg/g) for 4 h incubation in 5% CO_2 at 37 °C. After the medium was removed, the cells were washed three times with PBS (pH = 7.4) and the cover glass was visualized under a laser scanning confocal microscope (TCS SP5, Leica).

Cell Viability.

HeLa cells were cultured in DMEM supplemented with 10% fetal bovine serum (FBS), penicillin (100 units·ml^{-1}), streptomycin (100 mg·ml^{-1}) and 5% CO2 at 37 ℃. The viability of cells were investigated using 3-[4,5-dimethylthialzol-2-yl]-2,5-diphenyltetrazolium bromide (MTT, Sigma) assay. The assay was carried out in triplicate in the following manner. The cells were then incubated with various concentrations of DOX loaded PZNs, drug-free PZNs and free DOX for 24 h. Afterwards, cells were incubated in media containing 0.5 mg·mL^{-1} of MTT for 4 h. The precipitated formazan violet crystals were dissolved in 100 μL of 10% SDS in 10 mmol HCl solution at 37 °C overnight. The absorbance was measured at 470 nm by multi-detection microplate reader (680, BioRad Instruments Inc, USA).

Characterization.

X-ray diffraction (XRD) measurements were performed on a Shimadzu XRD-6000 powder X-ray diffractometer, using Cu Kα (λ = 1.5405 Å) as the incident radiation. Quantitative evaluation of the metal ion in the porous PZNs was conducted by using inductively coupled plasma (ICP) emission analysis equipment (Perkin-Elmer Optima 3000 DV). Transmission electron microscopy (TEM) samples were prepared by dropping the samples dispersed in water onto carboncoated copper grids with excess solvent evaporated. TEM images were recorded on a Shimadzu JEM-2010 CX with an accelerating voltage of 100 kV. The surface analysis was performed by nitrogen sorption isotherms at 77 K with amicromeritics ASAP2020 sorptometer. The surface areas were calculated by the Brunauer- Emmett-Teller (BET) method, and the pore size distributions were calculated by the Barrett-Joyner-Halenda (BJH) method. The measurement of the infrared spectroscopy was performed using a Nicolet IR100 infrared spectrometer. Thermo-gravimetric analysis (TGA) was performed on a NETZSCH STA 449 C TGA instrument at a heating rate of 20 ℃•min^{-1} in a nitrogen flow from 100 to 750 ℃. The zeta potentials were measured by a Malvern Nano-HT Zetasizer. Hydrodynamic diameters were determined using a BI-200SM dynamic light scattering device (DLS, Brookhaven Instruments Co.).UV-Vis absorption spectra were obtained by a UV-3600 spectrophotometer (Shimadzu). Solid-state UV spectra were taken on a Shimadzu UV-2450 spectropolarimeter.

Results and discussions

Characterization of the porous ZnS nanospheres carrier based on coordination bonding.

As shown in the TEM images (Figure 2A), the prepared PZNs were uniform spherical nanospheres with a mean diameter of approximately 60 nm. Detailed structural and crystallinity information was obtained from high-resolution TEM analysis as shown in Figure 2 (B). The porous structure is clearly observed, and was apparently assembled by small primary particles with a diameter of about 5 nm. The primary particles display high crystallinity with clear lattice fringes. The experimental lattice spacing of 0.31 nm is analogous to the (111) plane of cubic ZnS. The XRD patterns in Figure 2 (C) match well with the standard pattern of cubic zinc blend structure of

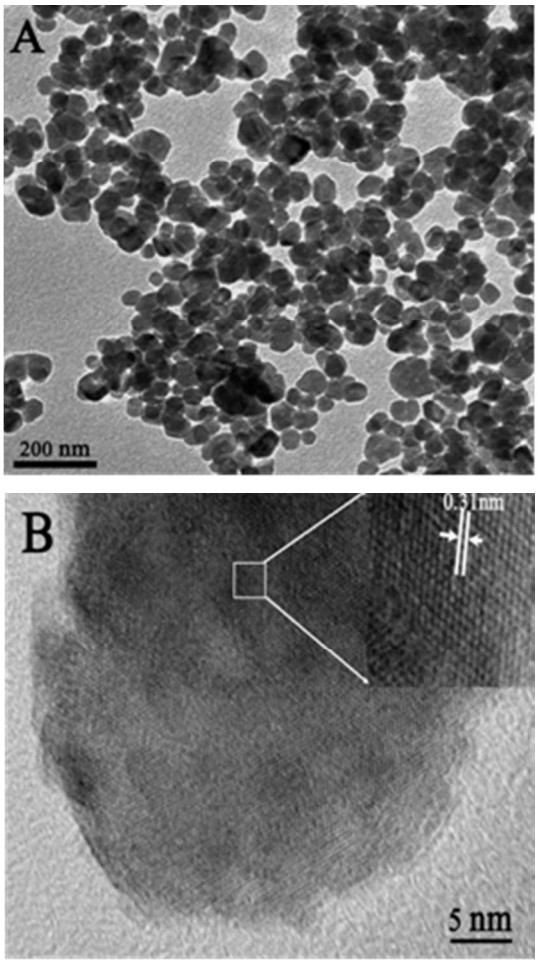

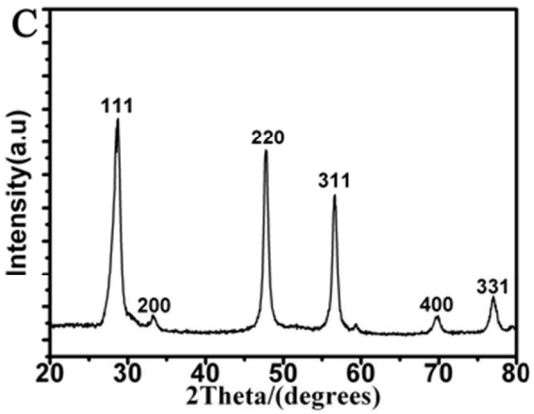

Figure 2 (A) Typical TEM image, (B) high-resolution image and (C) XRD patterns of PZNs.

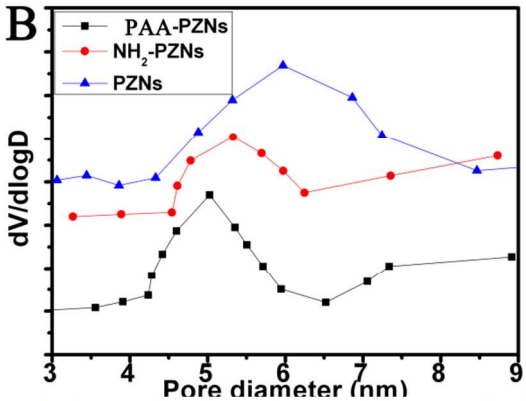

Figure 3 (A) N_2 adsorptiondesorption isotherms and (B) pore-size distribution of PZNs, NH_2-PZNs and PAA-PZNs

ZnS (JCPDS file No. 01-0792). Calculations using the Debye–Scherrer formula for the strongest peak (111) showed grain sizes of 6.8 nm, which is in good agreement with the TEM result.

N_2 absorption and desorption analysis was used to further examine the porous structure of PZNs, NH_2-PZNs and PAA-PZNs, as shown in Figure 3. The BET isotherms of these three materials (Figure 3A) both exhibited the characteristic type of IV curves with a hysteresis loop generated by capillary condensation according to the IUPAC classification, which indicated that both of them possess uniform porous channels. Despite that the adsorbed nitrogen amount of NH_2-PZNs and PAA-PZNs were reduced respectively, the shape of the hysteresis loop remained unchanged, which indicated that the pore shape was not significantly changed after successively grafting with cysteamine and PAA. The specific surface area and pore volume of PZNs were determined to be about 138 $m^2 g^{-1}$ and 0.45 $cm^3 \cdot g^{-1}$, respectively. The relatively large surface area and pore volume strongly support the fact that the nanospheres have a porous structure, which is attractive for loading drugs and the following sustained release. After

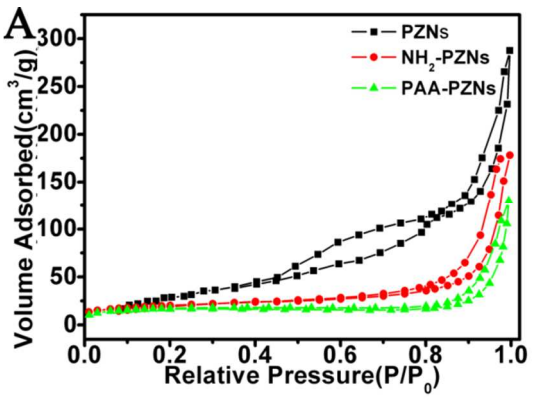

grafting with cysteamine and PAA subsequently, the surface area of NH_2-PZNs and PAA-PZNs were decreased to 75 $m^2 \bullet g^{-1}$ and 38 $m^2 \bullet g^{-1}$, respectively, and the corresponding pore volume were also decreased to 0.31 $cm^3 \bullet g^{-1}$ and 0.21 $cm^3 \bullet g^{-1}$. This is because some of the channel entrances could be covered respectively by the cysteamine and PAA chains in the drying treatment process. Furthermore, the average pore size was also decreased from 6.0 nm for PZNs to 5.1 nm for PAA-PZNs (Figure 3B), which also suggested that a portion of the PAA chains was grafted onto the internal surface of PZNs.

The Fourier transform infrared (FT-IR) spectra of the PZNs, NH_2-PZNs and PAA-PZNs were shown in Figure 4 (A). In contrast to that of the as-prepared PZNs, the FT-IR spectrum of amine functionalized PZNs displays a new peak at 3500 cm^{-1}, ascribed to the N-H stretching vibration. Moreover, a new peak assigned to N-H asymmetric bending vibration at 1559 cm^{-1} and two peaks assigned to C-H stretching vibrations at 2951 and 2887 cm^{-1} appeared which confirmed the successful functionalization of PZNs with amino groups. After grafting with PAA, two new adsorption peaks appeared at 1653 and 1717 cm^{-1}, which could be assigned to the C=O stretching vibration in the amide group, and the C=O stretching vibration in the carboxyl group, respectively, which indicated the successful grafting of PAA. This was also confirmed by the zeta potential measurement. In comparison with the PZNs (-9.2 mV), the zeta potential of the NH_2-PZNs was increased to 7.5 mV due to the loading of positively charged amine groups. After grafting with PAA, the zeta potential of PAA-PZNs was decreased to -50.3 mV, which indicated the existence of a great amount of carboxyl groups. All these results suggested that the PAA chains were successfully grafted onto PZNs.

The grafted amount of PAA on PZNs was estimated by TGA. The thermograms of PZNs, NH_2-PZNs and PAA-PZNs are shown in Figure 4 (B). In the tested temperature range (50 – 600 ℃), PZNs, NH_2-PZNs, and PAA-PZNs showed a weight loss of 11.8 wt %, 18.8 wt%, and 30.5 wt %, respectively. Thus, the graft ratio of PAA could be calculated to be about 11.7 wt %. The amounts of subsequently loading Zn^{2+} ions have also been calculated as 2.5 mmol/g by ICP analysis results.

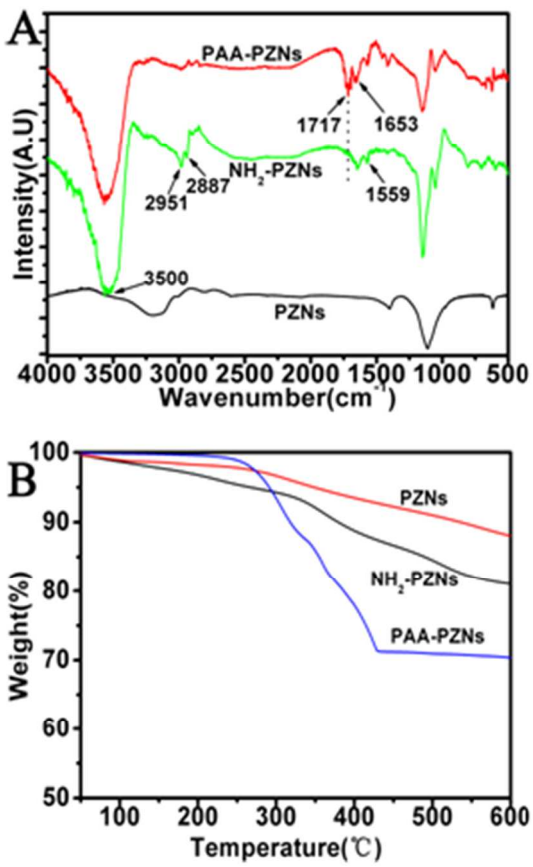

Figure 4 (A) FT-IR spectra of PZNs, NH_2-PZNs, and PAA-PZNs (B) TGA curves of PZNs, NH_2-PZNs, and PAA-PZNs.

High Drug Loading Efficiency.

DOX have amino, carbonyl, and hydroxyl groups which serve as binding sites to Zn^{2+} ions on the PAA-PZNs. The drug loading capacity of "Zn^{2+}-PAA-PZNs" at different weight ratio of "DOX/Zn^{2+}-PAA-PZNs" was listed in Table 1. The loading content and the entrapment efficiency of drug increased quickly with the increase of "DOX/ Zn^{2+}-PAA-PZNs" and could reach up to 60.9 mg/g and 95.2%, respectively, at "DOX-Zn^{2+}-PAA-PZNs" = 1. These results indicate that the carrier possess high drug loading efficiency to DOX.

Table 1 DOX loading content and entrapment efficiency of Zn^{2+}-PAA-PZNs

DOX/Zn^{2+}-PAA-PZNs	loading content (mg/g)	Entrapment efficiency (%)
0.2	21.5	85.2
0.4	39.6	90.2
0.6	57.3	93.2
0.8	60.3	95.4
1.0	60.9	95.2

pH-Responsive Release of DOX.

Figure 5 shows the release of DOX from DOX-Zn^{2+}-PAA-PZNs architectures with different pH solution. No significant release of the DOX from the PZNs carriers has been observed under the physiological pH (7.4) at 37℃, however, under mildly acidic conditions, drugs are released in significant amounts from the carrier into the external environment. The drug release rate was obviously pH dependent and increased with the decrease of pH, and the cumulative release amount of DOX could reach up to 91% after 24 h at pH 5.6, much higher than that at pH 6.2, 6.8 and 7.4, which was 70%, 36% and 12%, respectively. This is because the cleavage of the "COOH-Zn^{2+}-DOX" coordination bonds is sensitive to external pH variations. Both metal ions Zn^{2+} and protons (H^+) are Lewis acids and compete to combine with the carboxyl group, which is a Lewis base, while DOX and PAA on the carrier have the carboxyl groups. So, a breakup of either (or both) the "COOH-Zn^{2+}-DOX" coordination bond would occur, triggered by a reduction in external pH, leads to the release of drug molecules from the carrier into the surrounding environment. This mechanism can be found in nature, e.g., in the transferring recycling in cells.[42] Fe ions are transferred from the extracellar environment into the cytoplasm by the formation and breakage of coordination bonds in response to a pH change.

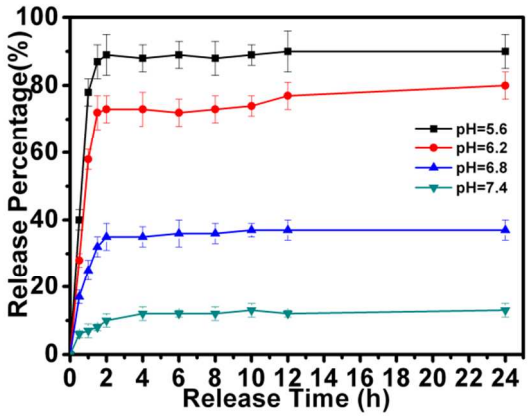

Figure 5 Release profiles of DOX-Zn^{2+}-PAA-PZNs with pH 5.6, 6.2, 6.8 and 7.4 at 37℃.

The solid-state UV-vis spectral results confirmed the break-up of the "Zn^{2+}-DOX" coordination bond. As shown in Figure 6, The peak around 495 nm belonging to the complex of "Zn^{2+}-DOX" has been observed in a set of DOX loaded "Zn^{2+}-PAA-PZNs" materials and the samples after releasing in PBS pH 7.4 for 12 h, indicating the formation and stability of the coordination bond of "Zn^{2+}-DOX". However, after releasing in PBS pH 5.6 for 12 h, the blue shift of the band from 495 to 478 nm belonging to DOX demonstrated the existence of the free DOX molecules instead of the "Zn^{2+}-DOX" complex, indicating the cleavage of the coordination bond between Zn^{2+} and DOX even under weakly acidic condition (pH = 5.6).

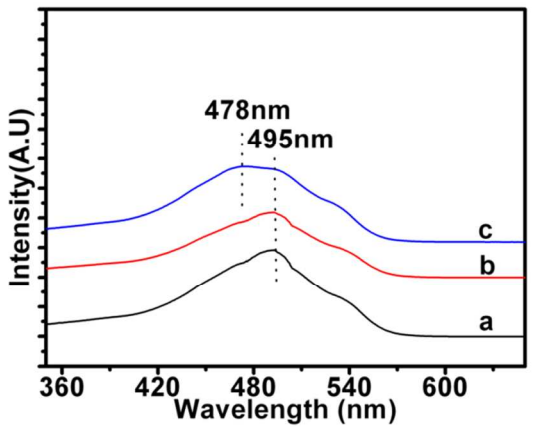

Figure 6. Solid-state UV-vis adsorption spectra of "DOX-Zn^{2+}-PAA-PZNs" systems treated in PBS solutions at different pH values. (a) As prepared DOX-Zn^{2+}-PAA-PZNs, (b) the sample in PBS pH 7.4 for 12 h, (c) the sample in PBS pH 5.6 for 12 h.

Table 2 shows the release of Zn^{2+} from the DOX-Zn^{2+}-PAA-PZNs hybrids with different pH solution. When the DOX-Zn^{2+}-PAA-PZNs hybrids were immersed in PBS of pH 5.6, the loss of the Zn^{2+} loading amount increased dramatically (Table 2), confirming that the cleavage of the "Zn^{2+}-COOH" coordination bonds, which induces to the significant release of model drug in the form of DOX or Zn^{2+}-DOX composites from the hybrid under low pH conditions. On the other hand, at pH 7.4, the diffusion kinetics of the Zn^{2+} ions was much slower and the hybrids maintained a relatively high loading amount of Zn^{2+}, which avoids significant release of the drug under physiological conditions. Considering the Zn^{2+} could be released from the intrinsic PZNs, we also performed the Zn^{2+} release control experiments with bared PZNs under pH 7.4 and pH 5.6. As shown in Table 2, released Zn^{2+} amounts from the bared PZNs were negligible, compared with the DOX-Zn^{2+}-PAA-PZNs hybrids. Thus, the cleavage of both sides of the "COOH- Zn^{2+}-DOX" architecture gave rise to a significant release of DOX under low pH conditions.

Table 2 Released Zn^{2+} amount from DOX-Zn^{2+}-PAA-PZNs architectures and bared PZNs

	Zn^{2+} amount from DOX-Zn^{2+}-PAA-PZNs architectures (μ mol/g)	Zn^{2+} amount from bared PZNs (μ mol/g)
0 h	0	0
pH 7.4, 1 h	54	3
pH 7.4, 8 h	78	5
pH 7.4, 20 h	107	8
pH 5.6, 1h	172	5
pH5.6, 8h	238	13
pH5.6, 20h	251	15

Calculated from ICP.

A control experiment without metal ions coordination bonding was also carried out and revealed that the drug release of DOX-PAA-PZNs was also slightly pH dependent. This is because the DOX will bind with the PAA to form the DOX-PAA-PZNs complex by the electrostatic interaction at pH 7.4. With the decrease of pH, more and more of the PAA was protonized, which would lead to the dissociation of electrostatic interaction between PAA and DOX, so that more of the DOX was released, which is similar to previous report.[43] However, compared to the DOX-Zn^{2+}-PAA-PZNs with metal ions (Zn^{2+}) coordination bonding, as shown in Figure 7, the released drug amount of DOX-PAA-PZNs could reach only 40%, 32%, 26% and 14% in corresponding PBS buffer after 24 h, respectively, which indicated that the release amount is quite small and that the difference in release amount between different pH is not significant. It was apparent that DOX-Zn^{2+}-PAA-PZNs exhibited a more pronounced pH-dependent drug release behavior than DOX-PAA-PZNs.

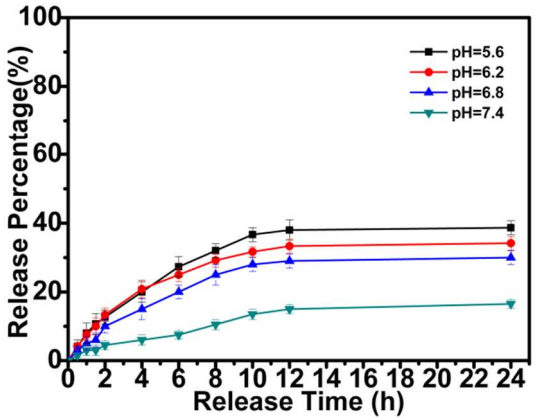

Figure 7. Release profiles of DOX-PAA-PZNs with pH 5.6, 6.2, 6.8 and 7.4 at 37℃ without Zn^{2+} coordination bonding.

The stability was also evaluated by monitoring their hydrodynamic size in the complete cell medium DMEM containing 10% FBS over a four-day period. As shown in Figure S1,* the hydrodynamic size of DOX-Zn^{2+}-PAA-PZNs didn't show major changes after 96 h, indicating the relatively higher stability of these nanospheres in biological fluids at physiological pH values.

In Vitro Cell Assay.

The cellular uptake and intracellular release behaviors were investigated by confocal laser scanning microscopy (CLSM). After incubation of HeLa cells with DOX-Zn^{2+}-PAA-PZNs hybrids for 4 h, the hybrids were rapidly internalized into the cells and localized mainly in the cytoplasm and subcellular vesicles, as indicated by the clearly bright-field image and visible red fluorescence of DOX (Figure 8 (A) and (B)). As shown in Figure 8, a remarkable intracellular fluorescence was also found localized in the nucleus of the cell, which suggests part of the loaded DOX released from the PZNs to enter the nucleus. This evidence visually confirms that the DOX-Zn^{2+}-PAA-PZNs system could penetrate into living cells and also that the loaded DOX could be released from the nanospheres in the acidic environment of cancerous cell, consistent with DOX release out of a dialysis bag in the weakly acidic conditions in the above text.

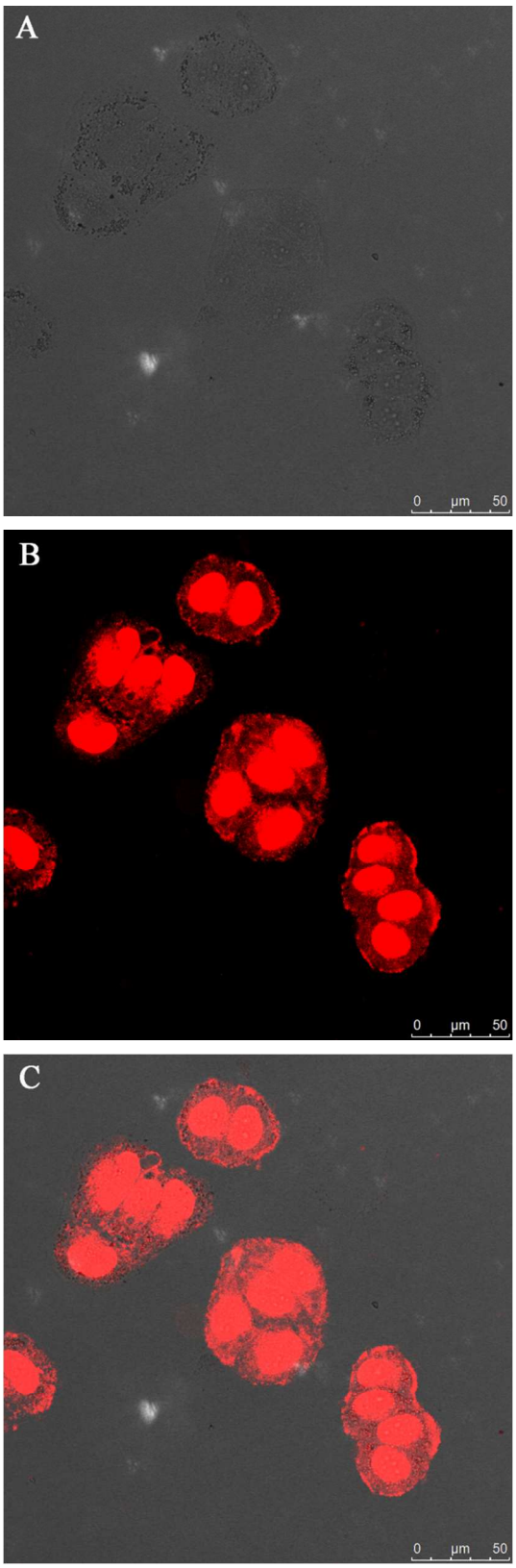

Figure 8. Fluorescence confocal images of "DOX-Zn^{2+}-PAA-PZNs" nanoparticles and their uptake by Hela cells. (a) Bright-field images; (b) fluorescence image excited at 480 nm; and (c) overlap image of (a) and (b).

An MTT assay was used for quantitative testing of the viability of HeLa cells in the presence of Zn^{2+}-PAA-PZNs, DOX- Zn^{2+}-PAA-PZNs and free DOX. As shown in Figure 9, Zn^{2+}-PAA-PZNs had no obvious effect on cell viability after they were incubated with the cells for 24 h, the cellular viability remained above 93% even up to doses of 96 μ g/mL. The viability studies also demonstrated that DOX-Zn^{2+}-PAA-PZNs greatly decreased the cell viability at concentrations as low as 6 μ g/mL, which is comparable to the cytotoxic effect of free DOX. Unlike free DOX, however, we expect that the Zn^{2+}-PAA-PZNs to deliver the cytotoxic agent selectively to the more acidic cancerous cells than to normal tissue.

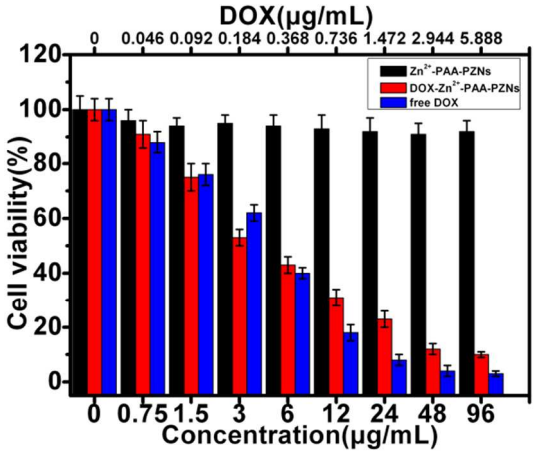

Figure 9. In vitro viability of HeLa cells in the presence of Zn^{2+}-PAA-PZNs, DOX-Zn^{2+}-PAA-PZNs and free DOX.

Conclusions

In summary, a pH-responsive release system was successfully constructed based on "COOH-Zn^{2+}-DOX" architecture via coordination bonding in ZnS nanospheres mesopores. PAA-functionalized PZNs material was used for hosting metal ion (Zn^{2+}) for further interaction with drug molecules. The formation and cleavage of coordination bonds have proved to be sensitive to pH variations. A breakup of either (or both) coordination bond, triggered by weakly acidic conditions (pH 5-6.5), resulted in release of the drug cargo from the pores of the PZNs into the surrounding environment. In view of the acidic exterior and interior environments of cancer cells, our system opens up a powerful route and new opportunities for pH-responsive drug delivery applications, especially for anticancer therapy.

Acknowledgements

We greatly appreciate the National Natural Science Foundation of China for the financial support (21205064). This work was also supported by Fund of State Key Laboratory of Analytical Chemistry for Life Science (SKLACLS1208).

Notes and references

1 V.P.Torchilin, *Nat. Rev. Drug Discovery*, 2005, **4**, 145.
2 E.R.Gillies and J. M. J. Fruechet, *Drug Discovery Today*, 2005, **10**, 35.
3 M. J. Vicent and R.Duncan, *Trends Biotechnol*, 2006, **24**, 39.
4 S.D.Brown, P.Nativo, J. Smith, D.Stirling, P.R.Edwards, B.Venugopal, D. J.Flint, J.A. Plumb, D.Graham and N.J. Wheate, *J. Am.Chem. Soc*, 2010, **132**, 4678.
5 C. E. Ashley, E.C. Carnes, G. K. Phillips, D.Padilla, P.N. Durfee, P. A. Brown, T. N. Hanna, J.W. Liu, B. Phillips, M. B. Carter, N. J. Carroll, X.M. Jiang, D. R. Dunphy, C. L. Willman, D.N. Petsev, D. G. Evans, A.N. Parikh, B.Chackerian, W. Wharton, D.S. Peabody and C. J. Brinker, *Nat. Mater*, 2011, **10**, 389.
6 I. I.Slowing and B.G.Trewyn, S.Giri, V. S. Y. Lin, *Adv. Funct. Mater.* 2007, **17**, 1225.
7 T.Hyeon, J. E.Lee, N.Lee, H.Kim, J. Kim, S.H.Choi, J.H. Kim, T. Kim, I. C.Song, S. P.Park and W.K.Moon, *J. Am. Chem. Soc.* 2010, **132**, 552.
8 S.Angelos, Y.-W.Yang, K. Patel, J. F.Stoddart and J. I.Zink, *Angew. Chem., Int. Ed*. 2008, **47**, 2222.
9 C.Park, K.Oh, S. C.Lee and C.Kim, *Angew. Chem., Int. Ed.* 2007, **46**, 1455.
10 C.-H.Lee, L.-W.Lo, C.-Y.Mou and C.-S.Yang, *Adv. Funct. Mater*. 2008, **18**, 3283.
11 C.B. Gao, H.Q. Zheng, L. Xing, M.H.Shu and S.A.Che, *Chem. Mater*. 2010, **22**, 5437.
12 H.Q.Zheng, Y. Wang and S.A. Che *J. Phys. Chem. C*, 2011. **115 (34)**, 16803.
13 H.Q.Zheng, C.B. Gao, B.W. Peng, M.H. Shu and S.A. Che. *J. Phys. Chem. C*, 2011, **115**, 7230.
14 T. D.Nguyen, K. C.-F. Leung, M.Liong, Y.Liu, J. F.Stoddart, J. I. Zink, *Adv. Funct. Mater*. 2007, **17**, 2101.
15 C.Park, K.Lee and C.Kim, *Angew. Chem., Int. Ed*. 2009, **48**, 1275.
16 R.Casasus, E.Climent, Ma.D. Marcos, R.Martı´nez-Manez, F. Sancenon, J.Soto, P.Amoros, J.Cano and E.Ruiz, *J. Am. Chem. Soc.* 2008, **130**, 1903.
17 Y.Zhu, J.Shi, W.Shen, X.Dong, J.Feng, M.Ruan and Y.Li, *Angew. Chem., Int. Ed.* 2005, **44**, 5083.
18 C.-Y. Lai, B. G.Trewyn, D. M. Jeftinija, K.Jeftinija, S.Xu, S.Jeftinija and V. S.-Y.Lin, *J. Am. Chem. Soc.* 2003, **125**, 4451.
19 Y.Qiu and K. Park, *Adv. Drug Delivery Rev.* 2001, **53**, 321.
20 Z. Zhou, S. Zhu and D.Zhang, *J. Mater. Chem.* 2007, **17**, 2428.
21 A. Schlossbauer, J.Kecht and T.Bein, *Angew. Chem., Int. Ed.* 2009, **48**, 3092.
22 K. C.-F. Leung, C.-P. Chak, C.-M. Lo, W.-Y.Wong, S.Xuan and C. H. K. Cheng, *Chem. Asian J*. 2009, **4**, 364.
23 L. E. Gerweck, *Semin. Radiat. Oncol*. 1998, **8**, 176.
24 C.de las Heras Alarcon, S.Pennadam and C.Alexander, *Chem. Soc. Rev*. 2005, **34**, 279.
25 S.-M.Lee, H.Chen, C. M.Dettmer, T. V. O'Halloran and S. T. Nguyen, *J. Am. Chem. Soc*. 2007, **129**, 15096.
26 P.Gupt, K. Vermani and S.Garg, *Drug Discovery Today* 2002, **7**,569.
27 R.Casasus, E.Climent, M.D.Marcos, R.Martinez-Manez, F.Sancenon, J.Soto, P.Amoros, J.Cano and E.Ruiz, *J. Am. Chem. Soc*. 2008, **130,** 1903.
28 C.Park, K.Oh, S. C. Lee and C.Kim, *Angew. Chem., Int. Ed.* 2007, **46**, 1455.
29 S. Angelos, N. M.Khashab, Y.-W.Yang, A.Trabolsi, H. A. Khatib, J. F. Stoddart and J. I. Zink, *J. Am. Chem. Soc.* 2009, **131**, 12912.
30 D. Zhu, X.X. Jiang, C. Zhao, X.L Sun, J-R Zhang and J-J Zhu, *Chem. Commun*. 2010,**46**, 5226.
31 D. Zhu, Y. Chen, L.P Jiang, J. Geng, J-R Zhang and J-J Zhu, *Anal. Chem*., 2011, **83**, 9076.
32 M. Hafeez, U. Manzoor and A. S. Bhatti, J. *Mater. Sci.: Mater. Electron*., 2011, **22**, 1772.
33 D. Zhu, W.Li, H.-Mei Wen, J-R. Zhang and J-Jie Zhu. *Anal. Methods*, 2013, **5**, 4321.
34 D. Zhu, W. Li, L. Ma and Y. Lei, *RSC Adv*., 2014, **4**, 9372.
35 (a) P. Wu, Y. He, H.-F. Wang and X.-P. Yan, *Anal. Chem*., 2010, **82**, 1427.; (b) P. Wu and X.-P. Yan, *Chem. Soc. Rev*., 2013, **42**, 5489.; (c) Y. He, H.-F. Wang and X.-P. Yan, *Chem. – Eur. J*., 2009, **15**,5436.;(d) H.-F. Wang, Y. Li, Y.-Y. Wu, Y. He and X.-P. Yan, *Chem.- Eur. J*., 2010, **16**, 12988.; (e). Y. He, H.-F. Wang and X.-P. Yan, *Anal. Chem*., 2008, **80**,3832.; (f). H.-F. Wang, Y. He, T.-R. Ji and X.-P. Yan, *Anal. Chem*., 2009, **81**, 1615.; (g). P. Wu, L.-N. Miao, H.-F. Wang, X.-G. Shao and X.-P. Yan, *Angew. Chem., Int. Ed*., 2011, **50**, 8118.
36 J.-S. Chang, K. L. B. Chang, D.-F. Hwang, Z.-L.Kong, *Environ. Sci. Technol.* 2007, **41**, 2064.
37 Q. He, Z. Zhang, F. Gao, Y. Li and J. Shi, *Small*, 2010, **7**, 271.
38 Q. He, Z. Zhang, Y. Gao, J. Shi and Y. Li. *Small* 2009, **5**, 2722.
39 Y.-S.Lin and C. L. Haynes, *J. Am. Chem. Soc.* 2010, **132**, 4834.
40 R. M. Xing and S. H. Liu, *Nanoscale*, 2012, **4**, 3135.
41 S.K Li, Z.G Wu, W.H Li, Y.Liu, R.F. Zhuo, D. Yan, W. Juna and P.X Yan *Cryst.Eng.Comm*, 2013, **15**, 1571.
42 A.Dautry-Varsat, A.Ciechanover and H.F.Lodish, *Proc.Natl.Acad. Sci.* U.S.A. 1983, **80**, 2258.
43 L.Yuan, Q.Q. Tang, D.Yang, J. Z. Zhang, F.Y.Zhang and J.H.Hu. *J. Phys. Chem. C*, 2011, **115**, 9926.

